Environ Geochem Health (2025) 47:297
https://doi.org/10.1007/s10653-025-02593-8

ORIGINAL PAPER

Health risk assessment caused by external and internal exposure to radiation dose from naturally occurring radioactive materials in outdoor dust

Şeref Turhan

Received: 24 February 2025 / Accepted: 3 June 2025 / Published online: 4 July 2025

Abstract Outdoor dust (ODST), which is the main carrier of toxic elements in urban or industrial environments, is also one of the important sources causing public health problems. ODSTs in the production areas of coal-fired brick kilns generally consist of soil dust, brick dust and coal bottom ash. Therefore, these ODSTs contain naturally occurring radioactive materials (NORMs) such as terrestrial radionuclides in the uranium (^{238}U) and thorium (^{232}Th) decay chains and radioactive potassium (^{40}K). For the first time in this study, radiological health risks caused by the ionizing radiation doses from NORM in ODST samples collected from thirty-one lignite coal-burning clay brick factories in Türkiye were assessed for adult workers by estimating total annual effective dose (TAED) due to the external and internal exposure and the corresponding total lifetime cancer risk (TLCR). The elemental concentrations of uranium (U), thorium (Th) and potassium (K) obtained in mg/kg from an energy-dispersive X-ray fluorescence spectrometric analysis were converted to the corresponding activity concentrations in Bq/kg of ^{238}U, ^{232}Th and ^{40}K. The average activity concentrations of ^{238}U, ^{232}Th and ^{40}K in ODST samples were found to be 33.4 (9.9 to 132.1 Bq/kg), 39.4 (21.9 to 59.2 Bq/kg) and 458.9 (328.3 to 712.9 Bq/kg) Bq/kg, respectively, which were comparatively to the worldwide soil average values. The average values of TAED and TLCR were estimated as 84.3 µSv and 3.4×10^{-4}, respectively. Radiological evaluation revealed that adult workers are exposed to an additional dose of one-fourth of the TAED (366 µSv) from external and internal (excluding radon) exposures from natural radiation.

Keywords Outdoor dust · Clay brick factories · NORM · Radiological risk · Annual effective dose · Excess lifetime cancer risk

Introduction

With the dizzying rate of development of industry and technology and rapid urbanization, the release of large amounts of toxic air pollutants into the atmosphere continues to be a major global problem that affects human health, the environmental and the quality of air, soil, and water (Abedin & Khan, 2022; Cui et al., 2024; Din et al., 2024; Ekoa Bessa et al., 2024; Geng & Bai, 2024; Manisalidis et al., 2020; Wong et al., 2023). Intake of toxic air pollutants such as radioactive materials, heavy metals, industrial gases, volatile organic compounds, industrial solvents, polycyclic aromatic hydrocarbons, etc., into the human body through inhalation, ingestion, and dermal contact causes cancer, neurological, cardiovascular, and respiratory diseases, and other serious chronic human health problems (Achilleos et al., 2024; Wong et al.,

Ş. Turhan (✉)
Department of Physics, Faculty of Science, Kastamonu University, 37150 Kastamonu, Turkey
e-mail: serefturhan@ymail.com

2023). Soil is not only a significant reservoir for toxic pollutants but also serves as a means of transporting them to the respiratory system in the form of dust (Zakaly et al., 2024). Outdoor dusts (ODSTs), usually originating from surface soils, are dry, solid, and fine particles that can float in the air (Abedin & Khan, 2022; Dudu et al., 2018). ODSTs in urban and industrial areas are produced by natural processes (earthquakes, rain, floods, landslides, soil erosion, heat and turbulent air currents, etc.) and/or various anthropogenic activities (brick and cement production, vehicle transportation, building and road construction, building demolition, textile industries, etc.). They are released into the atmosphere and slowly settle from the atmosphere to ground (Abedin & Khan, 2022; Addo et al., 2020; Dudu et al., 2018). Thus, ODST, which is the main carrier of toxic air pollutants in the urban environment and industrial areas, is also one of the most important public health problems (Bourliva et al., 2016; Dytłow & Górka-Kostrubiec, 2021; Navarro-Ciurana et al., 2023).

Naturally occurring radioactive materials (NORMs) contain radionuclides in the uranium (^{238}U), thorium (^{232}Th), and actinium (^{235}U) decay series and radioactive potassium (^{40}K) (UNSCEAR, 2000). NORMs are released into the air in the form of ODST from many lithogenic and anthropogenic sources and contaminate air, water and soil (Abedin & Khan, 2022; Addo et al., 2020; Zakaly et al., 2024; Zivuku et al., 2023). When NORMs in dust are released into the atmosphere, some of the NORMs may accumulate on the soil surface or be carried by wind to distant areas on meteorological events and weather conditions (Yesilkanat & Kobya, 2021). Gamma rays emitted from NORMs deposited on the surface cause external radiation in humans, while internal exposures result from inhalation and ingestion of NORMs in ODST samples (UNSCEAR, 2000). NORMs taken into the body can settle in various organs and can continuously expose these organs to ionizing radiations (especially alpha- and beta-rays) from NORMs, depending on their effective half-life. Thus, exposure to ionizing radiation can damage cells, tissues, organs, and DNA and may adversely affect human health, such as deteriorating lung function and increasing the risk of cancer and cardiovascular death (Achilleos et al., 2024). For this reason, the determination of NORM contents and sources in dust (outdoor and indoor dust) samples is a prerequisite for the assessment of radiological risks related to human health and monitoring of environmental pollution. Determination of NORM contents in ODST (street, road, and desert dust) samples and indoor (homes, schools, etc.) dust samples and assessment of radiological health risks (RHRs) due to external and internal exposures have been carried out by many researchers (Abdullaev et al., 2013; Abedin & Khan, 2022; Addo et al., 2020; Al-Hamidawi, 2015; Al-Khazzar et al., 2024; Arimoto et al., 2005; Doering et al., 2019; El-Zohry & El-Zayat, 2019; Han & Park, 2018; Hanfi et al., 2021; Hmood et al., 2019; Khan et al., 2024; Mahdi et al., 2017; Obayes et al., 2019; Pham et al., 2017). However, research on NORM concentrations in dust samples from industrial areas has been rarely conducted (Abdullah et al., 2019; Dudu et al., 2018; Zivuku et al., 2023). Dudu et al. (2018) determined the activity concentrations of NORMs (^{238}U, ^{232}Th, ^{226}Ra, and ^{40}K) in dust samples collected from the West Rand mining area of South Africa using a gamma-ray spectrometry (GRS). Abdullah et al. (2019) studied the radioactivity levels of NORMs (^{238}U, ^{232}Th and ^{40}K) in quarry dust samples collected from eight locations throughout Kelantan using a GRS and estimated the related radiological risks. Zivuku et al. (2023) measured the activity concentration of NORMs (^{238}U, ^{232}Th, ^{226}Ra, ^{210}Pb, and ^{40}K) in particulate matter (PM) and soil samples collected from two mining towns of Karibib and Arandis in Namibia using a GRS and evaluated the radiological human health of the people around the mining sites.

Rapid population growth and urban development have increased the demand for building materials worldwide (Idrees et al., 2023). Clay brick is one of the most widely used building materials and is mainly used in the construction of exterior and interior walls in buildings (Idrees et al., 2023; Koroneos & Dompros, 2007; Turhan et al., 2024a). Approximately 1.3 trillion clay bricks are produced worldwide each year (Idrees et al., 2023). The dramatic increase in clay brick production has caused various negative environmental effects (Idrees et al., 2023; Koroneos & Dompros, 2007; Turhan et al., 2024a). In a coal-fired brick kiln (CFBK), approximately 80% of the ash during combustion is released into the atmosphere as fly ash, while the remaining 20% is characterized as bottom ash (BA) (Siraz et al., 2023). Kiln dust, as ODST on the soil surface of the brick production site, generally consists of

BA, fine brick fragments and burnt clay (Turhan et al., 2024a). When NORMs in ODST are released into the atmosphere, some of the NORMs may accumulate on the soil surface in the production site or be carried off-site and spread to nearby soils as a result of the local climate. Some of the material accumulated in the ODST layer on the soil surface will become airborne again when disturbed by wind and human activities such as vehicle movement, digging or walking, causing additional internal exposures to workers resulting from inhalation and ingestion of NORMs. According to our literature research, no study has been conducted on the determination of NORMs and the assessment of the RHRs in ODST dust in the production areas of CFBKs.

Keeping all these in mind, the main objectives of this study are: (1) to determine the NORM contents of ODST collected from the production sites of CFBKs and (2) to assess RHRs for adult workers exposed to ionizing radiation. For this, (1) the contents of uranium, thorium and potassium in ODST samples collected from the production areas of thirty-one CFKBs located in the Western Black Sea Region of Türkiye, which meets approximately one-third of Türkiye's brick needs, were analyzed by using an energy dispersive X-ray fluorescence (EDXRF) spectrometer, (2) these contents were converted into activity concentrations of ^{238}U, ^{232}Th and ^{40}K and (3) to assess RHRs, the annual effective doses which adult workers in each factory could receive due to external and internal radiation exposure and the corresponding lifetime cancer risks for twenty years were estimated based on the activity concentrations of these NORMs.

The novelties of this study are (1) for the first time, it draws attention and creates awareness and concern about the additional radiation dose that workers may be exposed to due to dust in workplaces such as brick factories in Türkiye, and (2) that the information obtained as a result of the study provides guidance for brick manufacturers or authorized institutions to take measures and regulations to minimize the potential danger from NORM and thus protect human health and the environment.

Material and methods

Sample collection and preparation

Thirty-one ODST samples were collected from thirty-one CFBKs shown on the map in Fig. 1. The first twenty-four ODST samples were collected from the CFBKs located in the Boyabat district of Sinop province, and the next seven ODST samples were collected from the CFBKs located in the Tosya district of Kastamonu province (Turhan et al., 2024a). Each ODST sample was collected by carefully sweeping an area from the production areas of the CFBK with plastic tools, and then put into impermeable polyethylene packages for storage (Turhan et al., 2024a). Then, each ODST sample was coded and transported to the Analysis Preparation Laborator and kept in an atmospheric environment until analysis (Turhan et al., 2024a). ODST samples were dried in a furnace at 110 °C for five hours. After being homogenized, approximately five grams of each sample was taken for analysis (Turhan et al., 2024a). CFBK dust samples were coded as ODST.

Sample analysis

The elemental analysis of U, Th and K in ODST samples was carried out using EDXRF spectrometry (Spectro Xepos, Ametek). The EDXR spectrometer has a thick binary Pd/Co alloy anode X-ray tube (50 kV, 60 W) (Turhan et al., 2024a). The system's spectral resolution is less than 155 eV (Turhan et al., 2024a). The specifications of the EDXRF spectrometry are presented in Table 1 (Spectro Ametek, 2025).

Activity concentration of NORM

The elemental concentrations of U, Th, and K analyzed in the ODST sample by EDXRF were transformed to activity concentrations of NORMs with the equation given below (Turhan et al., 2024b):

$$\mathrm{AC} = \frac{\ln 2}{T_{1/2}} \times \frac{E_C \times h(\%) \times N_{Av}}{W \times f} \quad (1)$$

where AC is the activity concentration (Bq/kg) of ^{238}U, ^{232}Th and ^{40}K; $T_{1/2}$ is the half-life of radionuclide (4.468×10^{9} y, 1.408×10^{10} y and 1.28×10^{9} y for ^{238}U, ^{232}Th and ^{40}K, respectively); E_C is the elemental concentration of U (mg/kg), Th (mg/kg) and K (%); h is the isotopic abundance (%) of each radionuclide in nature (99.2752%, 100% and 0.0117% for ^{238}U, ^{232}Th and ^{40}K, respectively) (Turhan et al.,

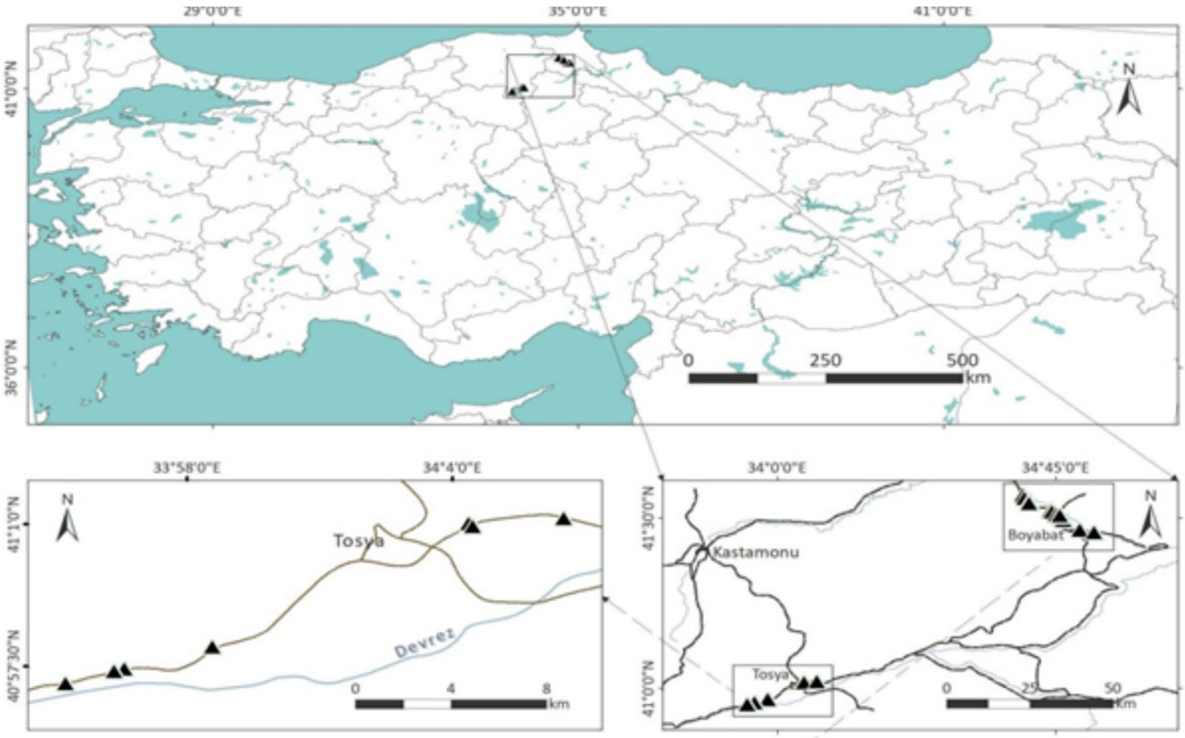

Fig. 1 Location of coal-fired brick kilns

Table 1 Specifications of EDXRF spectrometer

Excitation	• X-ray tube with thick binary Pd/Co alloy anode with air-cooling • Maximum power of 50 W • Maximum of 60 kV • Adaptive excitation system with optimized filters • Bandpass filter for improved performance for elements in the range K-Mn
Detection	• Silicon drift detector with Peltier cooling. It has delivered high resolution with low spectral • Large detector area (30 mm^2, active area 20 mm^2) • Spectral resolution (FWHM) ≤ 155 eV • Input count rate up to 1,000,000 counts/s • Detector filter changer for active pile-up reduction • Application range extended to multilayer analysis, up to 8 layers and up to 55 elements • No required calibration of certified reference samples. The user simply supplies relevant initial samples to build the database; the software examines the measured spectra and creates a fingerprint for each sample. Going forward, every newly introduced sample can be swiftly fingerprinted and compared to the rest of the database • Easy validation. Instead of validating each calibration for each element in each matrix, users simply check all samples of the database against each other and see the outcome

2010); N_{AV} is Avogadro's number (6.023×10^{23} atoms/mol); W is the atomic weight (kg/mol) and f is a factor with a value of 1,000,000 for ^{238}U and ^{232}Th, and 100 for ^{40}K (Turhan et al., 2010).

RHR assessment

Possible RHRs caused by the ionizing radiation emitted from NORMs in the ODST samples were assessed for adult workers, taking into account external and internal exposures.

External exposure

The contribution of gamma radiations from NORMs to the absorbed gamma dose rate (GDR) in outdoor air depends on the activity level of NORMs. Moreover, there is an instantaneous relationship between terrestrial gamma radiation dose and the activity concentrations of NORMs. When the activity concentration of NORMs is known, the GDR can be estimated. The outdoor GDR in the air at

Table 2 Elemental abundances and the corresponding activity concentrations in ODST samples with descriptive statistics

Sample code	Location	Elemental concentration (mg/kg)			Activity concentration (Bq/kg)		
		U	Th	K	^{238}U	^{232}Th	^{40} K
ODST1	Boyabat	1.3 ± 0.1	10.4 ± 0.4	18,450 ± 40	16.3 ± 0.8	42.2 ± 1.4	558.3 ± 17.9
ODST2		26.4 ± 0.7	14.8 ± 1.0	15,530 ± 30	102.5 ± 3.8	59.2 ± 1.4	469.9 ± 15.2
ODST3		1.2 ± 0.1	6.6 ± 0.3	14,500 ± 30	14.8 ± 0.7	26.8 ± 1.2	438.8 ± 14.1
ODST4		0.9 ± 0.2	10.7 ± 0.4	18,230 ± 40	11.1 ± 0.4	43.4 ± 1.6	551.6 ± 18.2
ODST5		1.3 ± 0.1	10.2 ± 0.4	18,530 ± 30	17.5 ± 0.7	41.4 ± 1.5	560.7 ± 19.2
ODST6		3.6 ± 0.2	11.2 ± 0.4	13,090 ± 30	44.4 ± 2.2	45.4 ± 1.8	396.1 ± 12.7
ODST7		0.8 ± 0.1	9.6 ± 0.3	18,070 ± 40	9.9 ± 0.3	38.9 ± 1.2	546.8 ± 18.4
ODST8		1.4 ± 0.1	8.1 ± 0.2	15,950 ± 30	17.3 ± 0.8	32.9 ± 1.8	482.6 ± 15.3
ODST9		3.6 ± 0.2	12.6 ± 0.4	15,990 ± 30	44.4 ± 1.9	51.1 ± 1.9	483.8 ± 15.5
ODST10		1.6 ± 0.1	8.9 ± 0.3	12,350 ± 30	19.8 ± 1.1	36.1 ± 1.3	373.7 ± 12.1
ODST11		1.3 ± 0.1	10.3 ± 0.4	15,350 ± 30	17..3 ± 0.8	41.8 ± 1.6	464.5 ± 14.8
ODST12		2.5 ± 0.2	12.1 ± 0.4	16,370 ± 30	30.9 ± 1.4	49.1 ± 1.8	495.3 ± 15.7
ODST13		1.3 ± 0.1	6.9 ± 0.3	13,950 ± 30	16.8 ± 0.7	27.2 ± 0.9	422.1 ± 13.5
ODST14		1.2 ± 0.1	9.6 ± 0.4	15,630 ± 30	14.8 ± 0.7	38.9 ± 1.1	472.9 ± 15.3
ODST15		12.7 ± 0.4	12.1 ± 0.4	18,900 ± 40	72.8 ± 2.9	46.6 ± 1.9	571.9 ± 18.7
ODST16		5.1 ± 0.3	13.1 ± 0.5	15,010 ± 30	64.2 ± 2.7	53.1 ± 2.0	454.2 ± 14.3
ODST17		1.6 ± 0.1	8.7 ± 0.4	14,600 ± 30	18.6 ± 1.0	35.3 ± 1.2	441.8 ± 14.2
ODST18		2.8 ± 0.1	7.5 ± 0.3	17,710 ± 30	34.6 ± 1.6	30.4 ± 1.1	535.9 ± 17.9
ODST19		1.5 ± 0.1	10.9 ± 0.4	16,740 ± 30	18.5 ± 0.9	44.2 ± 1.7	506.5 ± 16.1
ODST20		1.9 ± 0.1	8.7 ± 0.4	15,130 ± 30	23.5 ± 1.2	35.3 ± 1.7	457.8 ± 14.6
ODST21		4.7 ± 0.3	13.5 ± 0.5	23,560 ± 40	59.3 ± 2.7	54.8 ± 2.1	712.9 ± 22.6
ODST22		1.3 ± 0.1	5.4 ± 0.3	11,720 ± 30	16.3 ± 0.8	21.9 ± 0.7	354.6 ± 11.6
ODST23		1.5 ± 0.1	6.5 ± 0.3	15,920 ± 30	18.5 ± 0.8	26.4 ± 0.8	481.7 ± 15.3
ODST24		2.8 ± 0.2	8.5 ± 0.4	11,420 ± 30	34.6 ± 1.8	34.5 ± 1.3	345.6 ± 11.2
ODST25	Tosya	6.7 ± 0.1	11.1 ± 0.4	12,200 ± 30	82.7 ± 3.2	45.8 ± 1.8	369.2 ± 11.9
ODST26		20.7 ± 0.6	11.6 ± 0.8	11,880 ± 30	132.1 ± 5.7	47.1 ± 1.9	359.5 ± 11.4
ODST27		1.7 ± 0.1	6.2 ± 0.3	10,850 ± 30	19.8 ± 0.9	25.2 ± 0.8	328.3 ± 10.7
ODST28		1.4 ± 0.1	10.6 ± 0.5	14,970 ± 30	17.3 ± 0.6	42.6 ± 1.8	453.1 ± 14.5
ODST29		1.2 ± 0.1	9.1 ± 0.5	10,880 ± 30	14.8 ± 0.6	36.5 ± 1.3	329.2 ± 10.8
ODST30		1.3 ± 0.1	10.5 ± 0.5	15,480 ± 30	16.5 ± 0.8	42.6 ± 1.6	468.4 ± 14.9
ODST31		1.1 ± 0.1	6.3 ± 0.3	11,130 ± 30	13.6 ± 0.7	25.6 ± 0.8	336.8 ± 11.5
Average		2.7	9.7	15,164	33.4	39.4	458.9
Median		1.5	10.2	15,350	18.5	41.4	464.5
Standard deviation		2.4	2.3	2889	29.5	9.5	87.4
Standard error		0.4	0.4	519	5.3	1.7	15.7
Kurtosis		2.0	−0.02	0.6	2.0	−0.02	0.6
Skewness		3.6	−0.6	0.9	3.6	−0.6	0.9
Min		0.8	5.4	10,850	9.9	21.9	328.3
Max		10.7	14.6	23,560	132.1	59.2	712.9

1 m above the ground at each sampling point in the CFBK was estimated using the equation given below (UNSCEAR, 2000):

$$\text{GDR (nGy/h)} = \sum_i AC_i \times DCF_{iExt} \quad (2)$$

where AC_i is the activity concentrations (Bq/kg) of ^{238}U, ^{232}Th and ^{40}K, and DCF_{iExt} is the dose conversion factor (0.462, 0.604 and 0.0417 nGy/h per Bq/kg, respectively) (UNSCEAR, 2000). The corresponding annual effective dose (AED_{Ext}) was estimated as follows (UNSCEAR, 2000):

$$AED_{Ext}(\mu Sv/y) = GDR \times CF \times OF \times 10^{-3} \quad (3)$$

where GDR is the outdoor gamma dose rate given in Eq. (2), CF is the dose conversion factor of 0.7 Sv/Gy for adults, and OF is the outdoor occupancy factor of 0.2 (UNSCEAR, 2000).

Internal exposure

Internal exposures occur through the intake of NORMs in ODST samples by ingestion and inhalation (UNSCEAR, 2000). Annual effective dose (AED_{Ing}) due to the ingestion was estimated as follows (UNSCEAR, 2008, Turhan et al., 2024b):

$$AED_{Ing}(\mu Sv/y) = \sum_i AC_i \times EDC_{iIng} \times AI \quad (4)$$

where EDC_{iIng} is the effective dose coefficient for adult workers (0.044, 0.23 and 0.0062 µSv/Bq for ^{238}U, ^{232}Th and ^{40}K, respectively) (ICRP119, 2012) and AI is an annual intake of ODST (100 mg/d × 105 d/y) (USEPA, 2011).

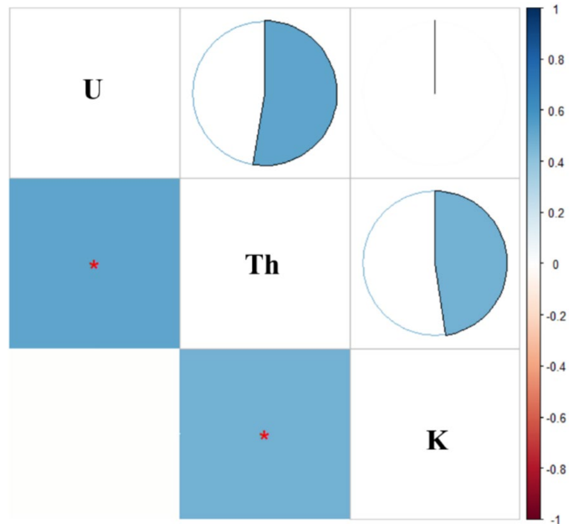

Fig. 3 Correlation plot for the transformed concentration of NORMs (*: significant correlations)

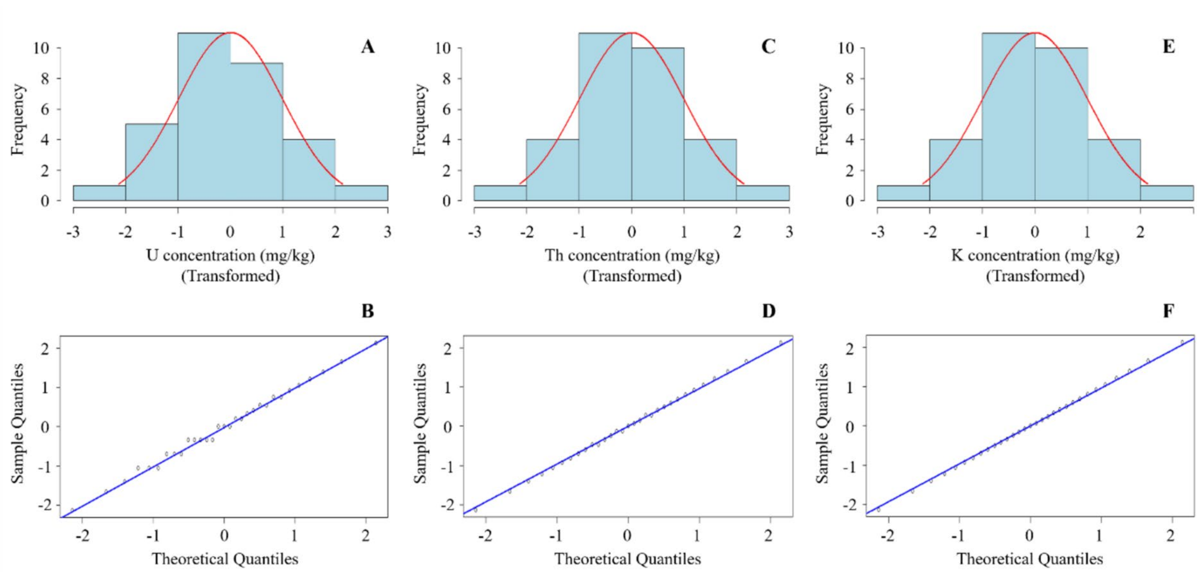

Fig. 2 The frequency distributions and Q-Q plots of the concentration of NORMs

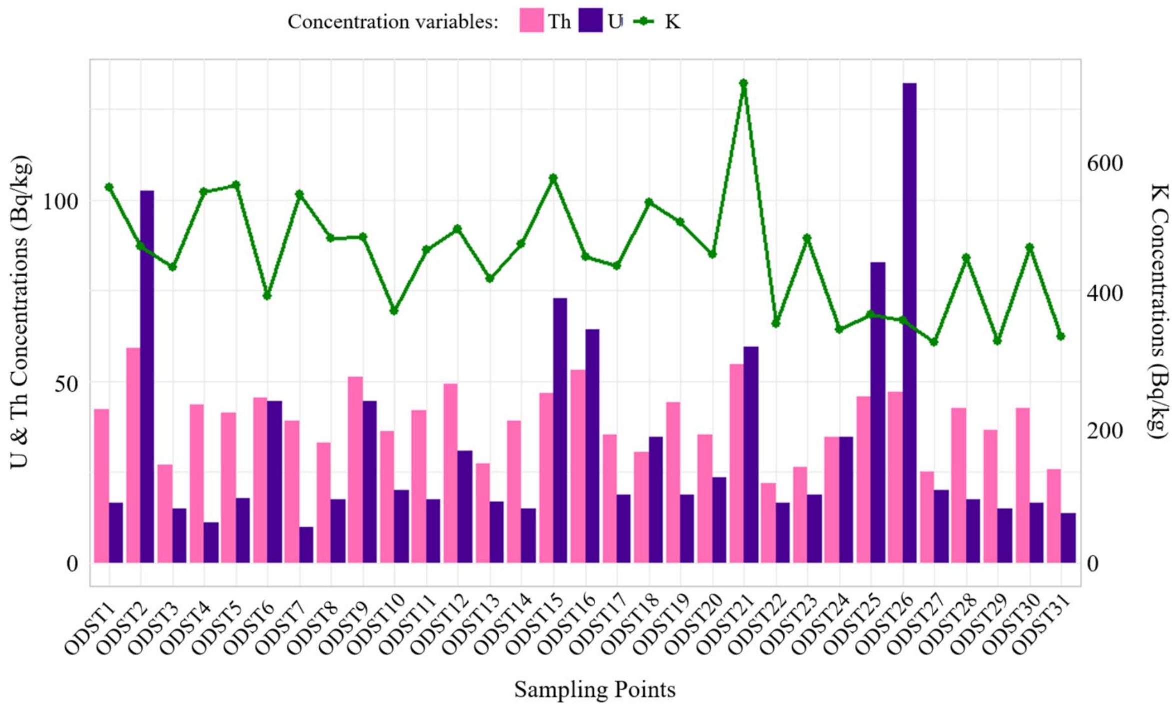

Fig. 4 Comparison of NORMs' distribution among the locations

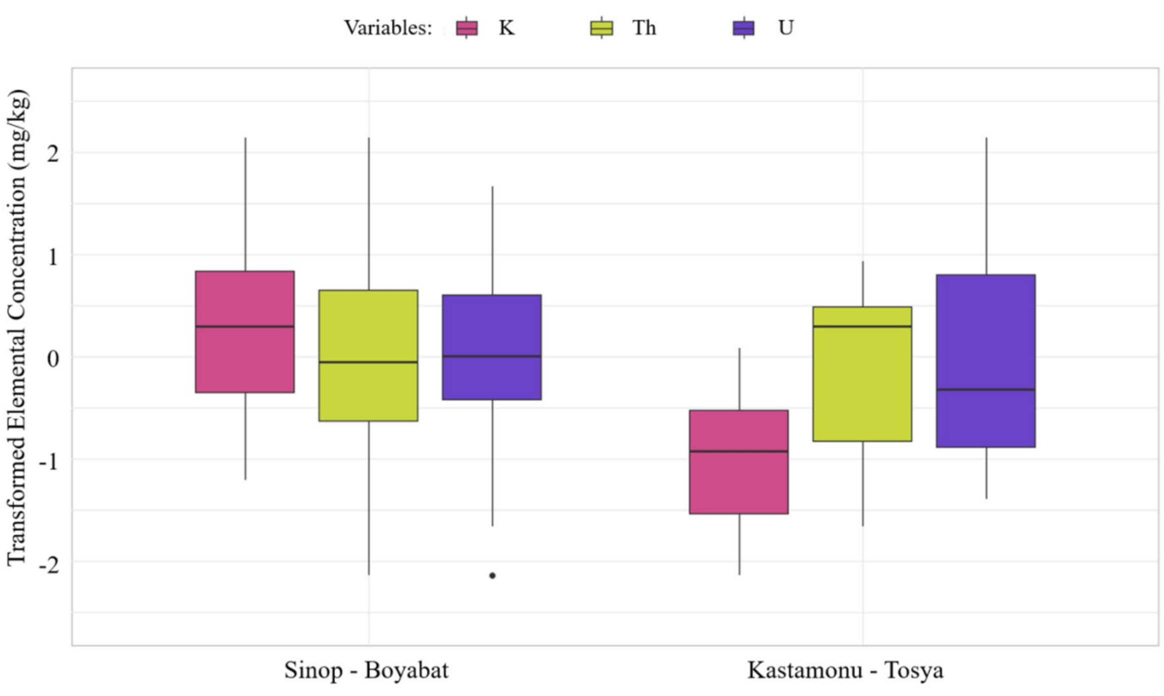

Fig. 5 Comparison of NORMs' according to the locations

Annual effective dose (AED_{Inh}) due to the inhalation was estimated as follows (UNSCEAR, 2008: Hanfi et al., 2021):

$$AED_{Ing}(\mu Sv/y) = \sum_i AC_i \times EDC_{iInh} \times V \times C \times T \quad (5)$$

where EDC_{iInh} is the effective dose coefficient for workers (1.6, 42 and 0.003 μSv/Bq for ^{238}U, ^{232}Th and ^{40}K, respectively) (ICRP119, 2012); V is breath frequency (20 m^3/d), and C is the average dust concentration (50 μg/m^3) (UNSCEAR, 2000) and T is the exposure time (20 y × 365 d/y).

Excess lifetime cancer risk

Total excess lifetime cancer risk (TLCR) caused by external and internal exposure annually was estimated as follows (ICRP, 1990):

$$TLCR = TAED \cdot ALT \cdot RF \quad (6)$$

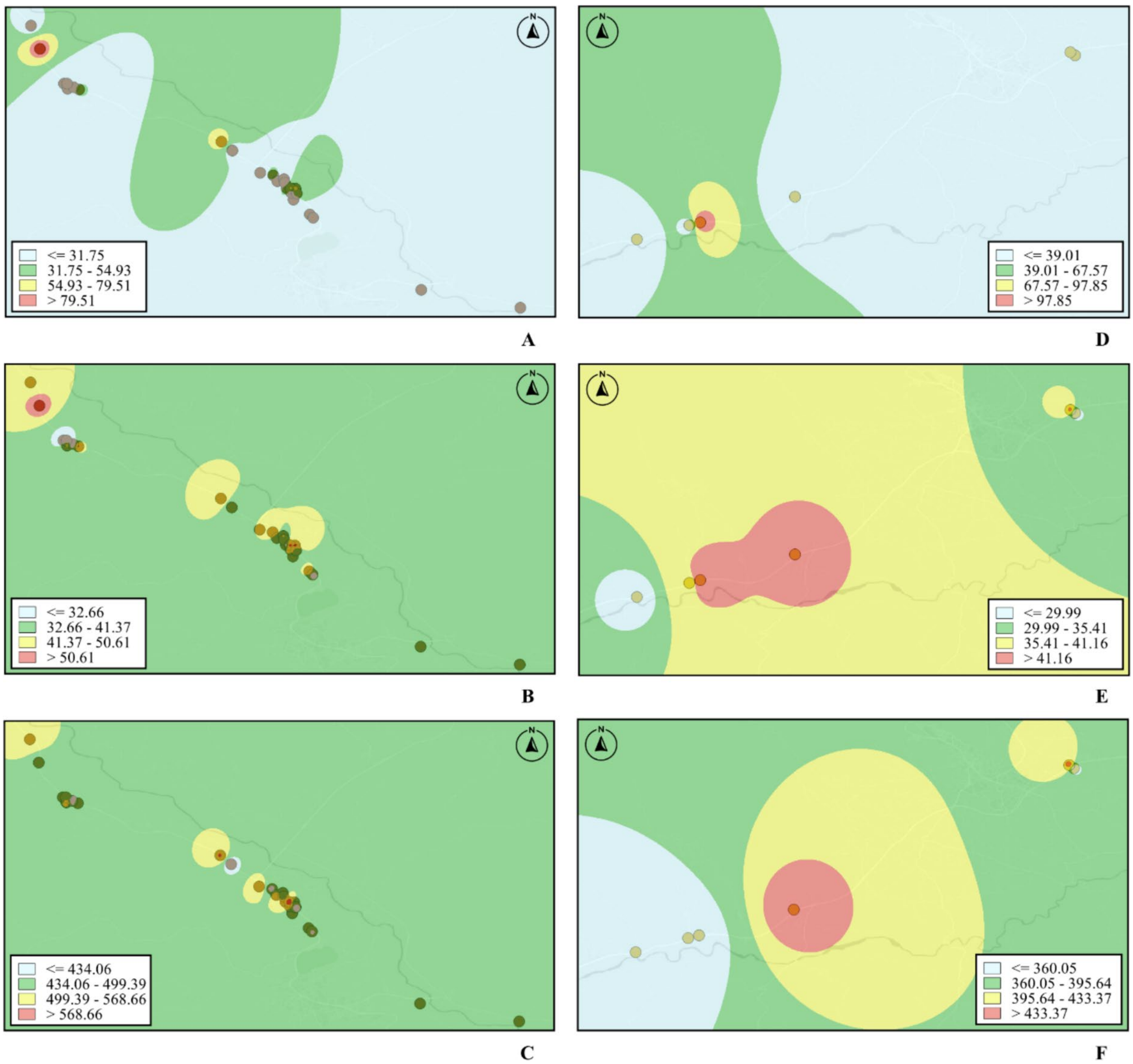

Fig. 6 The spatial distribution maps of the activity concentrations of NORMs in the ODST samples **A** U—Boyabat, **B** Th—Boyabat, **C** K—Boyabat, **D** U—Tosya, **E** Th—Tosya, **F** K—Tosya

Table 3 Radiological health risk parameter estimated for workers

Sample code	GDR (nGy/h)	Annual effective dose (μSv)				TLCR
		AED_{Ext}	AED_{Inh}	AED_{Ing}	TAED	
ODST1	56	69	13.15	0.15	82.4	3.3E-04
ODST2	103	126	19.38	0.22	145.6	5.8E-04
ODST3	41	51	8.40	0.10	59.2	2.4E-04
ODST4	54	67	13.46	0.15	80.3	3.2E-04
ODST5	56	69	12.91	0.14	82.4	3.3E-04
ODST6	64	79	14.47	0.16	93.8	3.7E-04
ODST7	51	62	12.08	0.13	74.7	3.0E-04
ODST8	48	59	10.29	0.12	69.3	2.8E-04
ODST9	72	88	16.21	0.18	104.2	4.2E-04
ODST10	47	57	11.32	0.12	68.5	2.7E-04
ODST11	53	65	13.03	0.14	77.7	3.1E-04
ODST12	65	79	15.43	0.17	94.8	3.8E-04
ODST13	42	51	8.54	0.10	59.9	2.4E-04
ODST14	50	61	12.13	0.13	73.7	2.9E-04
ODST15	86	105	15.18	0.18	120.5	4.8E-04
ODST16	81	99	17.06	0.19	116.3	4.6E-04
ODST17	48	59	11.06	0.12	70.5	2.8E-04
ODST18	57	70	9.75	0.12	79.4	3.2E-04
ODST19	56	69	13.79	0.15	83.1	3.3E-04
ODST20	51	63	11.11	0.13	74.1	3.0E-04
ODST21	90	111	17.51	0.21	128.4	5.1E-04
ODST22	36	44	6.92	0.08	50.6	2.0E-04
ODST23	45	55	8.32	0.10	63.1	2.5E-04
ODST24	51	63	10.99	0.12	74.0	3.0E-04
ODST25	81	100	15.04	0.17	115.0	4.6E-04
ODST26	104	128	15.99	0.20	144.4	5.8E-04
ODST27	38	47	7.95	0.09	54.7	2.2E-04
ODST28	53	65	13.28	0.14	78.0	3.1E-04
ODST29	43	52	11.38	0.12	63.8	2.5E-04
ODST30	53	65	13.27	0.14	78.3	3.1E-04
ODST31	36	44	8.01	0.09	52.0	2.1E-04
Average	58.4	71.6	12.5	0.14	84.3	3.4E-04
Min	35.5	43.6	6.9	0.08	50.6	2.0E-04
Max	104.4	128.2	19.4	0.22	145.6	5.8E-04

where TAED is the total annual effective dose rate and equal to the sum of AED_{Ext}, AED_{Ing} and AED_{Inh}, ALT denotes the average lifetime of 70 y, and RF is the cancer risk factor of 0.057/Sv (ICRP, 1990).

Spatial distribution analysis

NORM concentration distribution was examined using QGIS Desktop 3.36.0. The sampling locations' geographic coordinates were plotted on a digital platform. Inverse distance weighting (IDW) interpolation was applied to estimate radionuclide concentrations throughout the study area, utilizing measured values from the sampled sites.

Statistical analysis

Statistical analyses were performed to examine data distribution, assess variance homogeneity, and determine differences in NORM concentrations among groups. The Shapiro–Wilk test was used to evaluate normality, while the Levene test assessed variance homogeneity. Findings revealed that the data did not follow a normal distribution or meet the assumption of homogeneity. Various transformation techniques were explored, and rank transformation was chosen as it successfully normalized the distribution.

After achieving normality and variance homogeneity, an ANOVA test ($p = 0.05$) was conducted to analyze variations in NORM concentrations across locations. Additionally, Pearson correlation coefficients were calculated to identify relationships among NORMs. All statistical analyses were performed using R Studio version 2023.06 (R Core Team, 2023).

Results and discussion

NORM concentrations

Table 2 presents the elemental concentrations of U, Th, and K analyzed in each ODST sample, as well as the calculated activity concentrations of NORMs with some descriptive statistical data such as average, median, standard deviation, and error. The frequency distributions and Q-Q plots of the concentrations of NORMs are shown in Fig. 2. Figure 2 illustrates that the rank transformation successfully normalizes all NORM data. The Pearson correlation test results, presented in Fig. 3, indicate a significant positive correlation between U concentration and Th concentration, as well as between Th concentration and K concentration.

From Table 2, the average concentrations of U, Th and K analyzed in the ODST samples were 2.7 ± 0.4 (0.8–10.7) mg/kg, 9.7 ± 0.4 (5.4–14.6) mg/kg and 1.5 ± 0.1 (1.1–2.4) %, respectively. The average concentration of U is equal to that analyzed in the upper crust composition (UCC), while the average concentrations of Th and K were relatively lower than those (10.5 mg/kg and 2.3% for Th and K, respectively) in UCC (Rudnick & Gao, 2014).

The activity concentrations (ACs) of ^{238}U, ^{232}Th and ^{40}K in all ODST samples are given in Fig. 4. and it shows that ACs varied from 9.9 (ODST7) to 132 (ODST26) Bq/kg with an average of 33.4 ± 5.3 Bq/

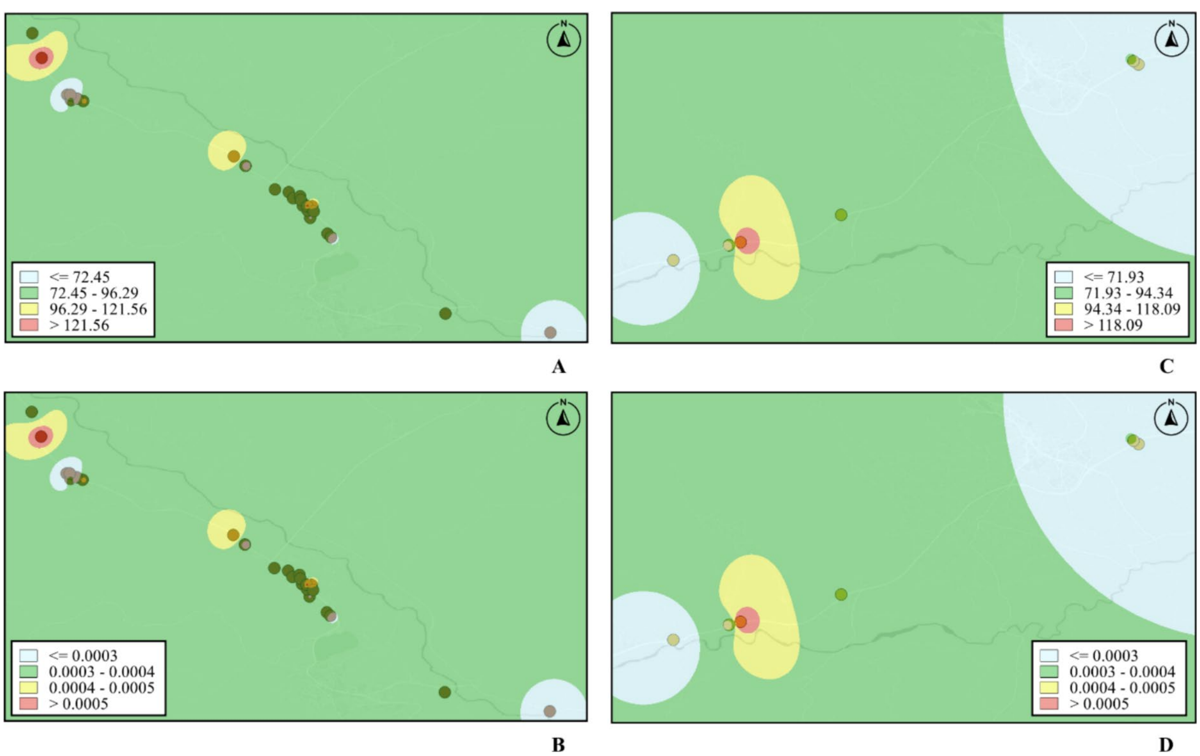

Fig. 7 The spatial distribution maps of TAED and TLCR for locations **A** TAED—Boyabat, **B** TLCR—Boyabat, **C** TAED—Tosya, **D** TLCR—Tosya

kg, 21.9 (ODST22) to 59.2 (ODST2) Bq/kg with an average of 39.4 ± 1.7 and 328.3 (ODST27) to 712.9 (ODST21) Bq/kg with an average of 458.9 ± 15.7, respectively. As shown, the variation in the activity levels of NORMs in the ODSTR samples could be due to local factors such as soil class and concentration dust loading of air from coal ash and brick dust. The average AC of ^{238}U was found to be very close to the current worldwide average (CWA) value of 33 Bq/kg (UNSCEAR, 2008). The average AC of ^{232}Th is below the CWA value of 45 Bq/kg, while the average AC of ^{40}K is higher than the CWA value of 412 Bq/kg (UNSCEAR, 2008). 32%, 29% and 71% of the ODST samples had ACs of U, Th and K above the quoted CWAs, respectively. However, the average ACs of NORMs in the ODST samples are greater than those (28.6, 33.0 and 448.5 Bq/kg for ^{238}U, ^{232}Th and ^{40}K, respectively) measured in surface soil samples from Türkiye (Turhan et al., 2012).

The variations in NORM concentrations between different locations, specifically Boyabat and Tosya, were examined using box plots (Fig. 5) and an ANOVA test. The ANOVA results indicated no statistically significant difference in U concentrations between the two locations ($p = 0.3169$) nor in Th concentrations ($p = 0.641$). However, a significant difference was observed in potassium (K) distribution between the two sites ($p = 0.00108$).

The spatial distribution maps of the activity concentrations of NORMs in the ODST samples obtained by inverse distance weighting (IDW) interpolation for Boyabat and Tosya are shown in Fig. 6.

Assessment of RHR

The values of the RHR parameters estimated for workers working in the CFBKs are given in Table 3. From Table 3, the GDR values varied from 35.5 to 104.4 nGy/h with an average value of 58.4 nGy/h, which is close to the world average outdoor absorbed gamma dose rate of 59 nGy/h (UNSCEAR, 2008). The corresponding AED_{Ext} values varied from 43.6 to 128.2 μSv/y with an average value of 71.6 μSv, which is also close to the world average outdoor annual effective dose of 70 μSv (UNSCEAR, 2008). The AED_{Inh} values varied from 6.9 to 19.4 μSv with an average value of 12.5 μSv, which is two times higher than the world average AED of 5.8 μSv from inhalation of ^{238}U and ^{232}Th series radionuclides in air (UNSCEAR, 2008). The AED_{Ing} values varied from 0.08 to 0.22 μSv with an average value of 0.14 μSv, which is well below the world average AED of 290 μSv from the ingestion of terrestrial radionuclides (UNSCEAR, 2008).

The values of TAED and the corresponding TLCR vary from 50.6 to 145.6 μSv with an average value of 84.3 μSv and 2.0×10^{-4} to 5.8×10^{-4} with an average value of 3.4×10^{-4}, respectively. These values are one-fourth of the world average value of 366 μSv from external (NORMs outdoors) and internal (inhalation and ingestion of NORMs) exposures and the corresponding excess TLCR of 1.5×10^{-3} (UNSCEAR, 2008). The distribution of TAED and TLCR values in Boyabat and Tosya are presented in Fig. 7.

Conclusion

For the first time, this study investigated the presence and levels of NORM concentrations in the outdoor dust of the production areas of coal-fired brick kilns in the region where the brick factories are most densely located in Türkiye and assessed the radiological health risks for workers exposed to external and internal irradiation resulting from these NORMs. In addition, this study emphasized the importance of characterizing industries containing NORM in terms of assessing radiological effects and implementing appropriate safety measures.

Consequently, this study may raise public awareness and attract the attention of relevant institutions regarding the radiological hazards of workers in the brick industry originating from NORMs in outdoor dust. Thereby, the following points were highlighted: (1) employers should use modern and effective technologies to minimize radiological health risks due to occupational exposure, (2) the use of personal protective equipment among employees should be made mandatory to limit NORM exposure, and (3) such workplaces should be regularly monitored.

Acknowledgements The author would like to thank Prof. Dr. Ergin Murat Altuner for his contribution to the statistical evaluations.

Author contributions The study was carried out by Seref Turhan.

Funding The authors have not disclosed any funding.

Data availability No datasets were generated or analysed during the current study.

Declarations

Conflict of interests The author declares that there is no competing financial interests or personal relationships that could have appeared to influence the study reported in this manuscript.

References

Abdullaev, S. F., Nazarov, B. I., Maslov, V. A., & Djuraev, A. A. (2013). Distribution of natural and anthropogenic radioactivity in samples of soil and dust haze in the South of Tajikistan. *Atmospheric and Oceanic Optics, 26*(5), 396–403.

Abdullah, A., Jaikol, E., Arshad, N., & Saat, A. (2019). Radiological assessments of quarry dust from quarries in Kelantan, Malaysia. AIP Conf. Proc. 2068.

Abedin, M. J., & Khan, R. (2022). NORMs distribution in the dust samples from the educational institutions of Megacity Dhaka, Bangladesh: Radiological risk assessment. *Journal of Hazardous Materials Advances, 8*, 1–13.

Achilleos, S., Henderson, C., Kouis, P., Achilleos, A., Argyrou, A., Caballero, A., Prokopiou, E., Kokkinofta, R., Savvides, C., Vasiliadou, E., Tzortzis, M., Sisou, A., Koutrakis, P., Yiallouros, P. K., & Quattrocchi, A. (2024). Airborne particle radioactivity during desert dust days in Cyprus. *Journal of Environmental Radioactivity, 278*, 1–8.

Addo, M. A., Lomotey, J. S., Osei, B., & Appiah, K. (2020). Measurement of natural radioactivity in soil dust samples along roadways in high commercial areas of the Ketu South district of the Volta Region, Ghana. *Radiation Protection and Environment, 43*, 6–12.

Al-Hamidawi, A. A. A. (2015). Evaluation of natural radioactivity in dust storms samples from Al-Najaf//Iraq. *Journal of Physical Science and Application, 5*(2), 143–146.

Al-Khazzar, A., Majid, H., & Al-Dulaimi, R. (2024). Natural radioactivity concentrations in air samples in Baghdad. *Turkish Journal of Nuclear Sciences, 37*(1), 1–6.

Spectro Ametek, (2025). White paper. Simple, easy, powerful identification software for XRF spectrometers. Web page: https://www.spectro.de/landingpages/xrf-wp-identification-software-for-xrf-spectrometers

Arimoto, R., Webb, J. L., & Conley, M. (2005). Radioactive contamination of atmospheric dust over southeastern New Mexico. *Atmospheric Environment, 39*, 4745–4754.

Bourliva, A., Papadopoulou, L., & Aidona, E. (2016). Study of road dust magnetic phases as the main carrier of potentially harmful trace elements. *Science of the Total Environment, 553*, 380–391.

Cui, Y., Fan, C., Zhou, X., & Peng, Y. (2024). Impact of urbanization on heavy metals in outdoor air and risk assessment: A case study in severe cold regions. *Sustainable Cities and Society, 114*, 1–16.

Din, I. U., Muhammad, S., Faisal, S., Rehman, I. U., & Ali, W. (2024). Heavy metal(loid)s contamination and ecotoxicological hazards in coal, dust, and soil adjacent to coal mining operations, Northwest Pakistan. *Journal of Geochemical Exploration, 256*, 1–12.

Doering, C., McMaster, S. A., & Johansen, M. P. (2019). Modelling the dispersion of radionuclides in dust from a landform covered by low uranium grade waste rock. *Journal of Environmental Radioactivity, 202*, 51–58.

Dudu, V. P., Mathuthu, M., & Manjoro, M. (2018). Assessment of heavy metals and radionuclides in dust fallout in the West Rand mining area of South Africa. *Clean Air Journal, 28*, 42–52.

Dytłow, S., & Górka-Kostrubiec, B. (2021). Concentration of heavy metals in street dust: An implication of using different geochemical background data in estimating the level of heavy metal pollution. *Environmental Geochemistry and Health, 43*, 521–535.

Ekoa Bessa, A. Z., Ganmo, K. M., Edjengte, D. E. P., Kayitesi, M. N., Ngnitedem, T. R. J., Tchadji, D. J. G., & Armstrong-Altrin, J. S. (2024). Assessment of heavy metals and radionuclides (U and Th) contamination, and source identification of the e Lékié Watershed sediments Cameroon. *Geosystems and Geoenvironment, 3*(1), 1–12.

El-Zohry, M. A., & El-Zayat, M. H. (2019). Radioactivity concentrations in dust and soil of enhanced occurring natural radionuclides and their transfer factors to urban trees in phosphate polluted area. *Arab Journal of Nuclear Sciences and Applications, 52*(4), 93–99.

Geng, X. S., & Bai, L. (2024). Characteristics of particulate matter and polycyclic aromatic hydrocarbon pollution generated during kitchen cooking and health risk assessment. *Indoor and Built Environment, 33*(4), 722–740.

Han, C. H., & Park, J. W. (2018). Analysis of the natural radioactivity concentrations of the fine dust samples in Jeju Island, Korea and the annual effective radiation dose by inhalation. *Journal of Radioanalytical and Nuclear Chemistry, 316*(3), 1173–1179.

Hanfi, M. Y., Yarmoshenko, I. V., & Zhukovsky, M. V. (2021). Assessment of radiation dose from inhalation of outdoor dust containing natural radionuclides. *Radiation Protection Dosimetry, 196*(3–4), 184–189.

Hmood, A. N., Alhesnawi, A., Hameed, A. S., & Ashour, N. I. (2019). Assessment of the natural radioactivity and concentrations of some heavy elements in the dust of some schools in Karbala, Iraq. *Iranian Journal of Medical Physics, 16*, 280–284.

ICRP .(1990). Recommendations of the International Commission on Radiological Protection, vol. 212, No.1–3, publication 60.

ICRP 119. (2012). Compendium of dose coefficients based on ICRP Publication 60. Ottawa.

Idrees, M., Akbar, A., Saeed, F., Gull, M., & Eldin, S. M. (2023). Sustainable production of Low-Shrinkage fired clay bricks by utilizing waste plastic dust. *Alexandria Engineering Journal, 68*, 405–416.

Khan, R., Habib, M. A., Tamim, U., Kormoker, T., Khan, M. H. R., Rashid, M. B., Idris, A. M., Aldawood, S., Hossain, S. M., & Islam, M. S. (2024). Fractionation of environmental radioactivity in road dust from a megacity: External and internal health risks. *Environmental Science and Pollution Research, 31*, 8254–8273.

Koroneos, C., & Dompros, A. (2007). Environmental assessment of brick production in Greece. *Building and Environment, 42*, 2114–2123.

Mahdi, K. H., Nassif, R. M., & Obayes, K. H. (2017). Radionuclides concentration and radiological risk in the dust rising in some streets of Diwaniyah City due to the movement of wheels and cars. *International Journal of Scientific Research, 6*(10), 1148–1154.

Manisalidis, I., Stavropoulou, E., Stavropoulos, A., & Bezirtzoglou, E. (2020). Environmental and health impacts of air pollution: A review. *Frontiers in Public Health, 8*(14), 1–13.

Navarro-Ciurana, D., Corbella, M., & Meroño, D. (2023). Effects of road dust particle size on mineralogy, chemical bulk content, pollution and health risk analyses. *International Journal of Environmental Research and Public Health, 20*(17), 1–26.

Obayes, K. H., Mahdi, K. H., Nassif, R. M., & Mansour, H. L. (2019). Determination of radionuclides and heavy elements in the rising dust in the small side of Diwaniyah city due to the movement of wheels and cars. *Journal of Physics: Conference Series, 1234*, 1–13.

Pham, M. K., Chamizo, E., Balbuena, J. L. M., Miquel, J. C., Martín, J., Osvath, I., & Povinec, P. P. (2017). Impact of Saharan dust events on radionuclide levels in Monaco air and in the water column of the northwest Mediterranean Sea. *Journal of Environmental Radioactivity, 166*, 2–9.

R Core Team. R: A language and environment for statistical computing. R Foundation for Statistical Computing, Vienna, Austria. https://www.R-project.org/. Accessed 2023

Rudnick, R.L., & Gao, S. (2014). Composition of the continental crust. The crust (ed. R.L.Rudnick), Treatise on geochemistry (eds. H.D. Holland and K.K. Turekian) , 2nd4. Elsevier-Pergamon, Oxford.

Siraz, M. M. M., Al Mahmud, J., Alam, M. S., Rashid, M. B., Hossain, Z., Khandaker, M. U., Bradley, D. A., Miah, M. M. H., Alshahrani, B., & Yeasmin, S. (2023). Risk assessment of naturally occurring radioactivity in soil adjacent to a coal-fired brick kiln. *Radiation Physics and Chemistry, 209*, 1–11.

Turhan, Ş, Altuner, E. M., Bakır, T. K., Duran, C., Hançerlioğulları, A., & Kurnaz, A. (2024a). Assessment of human health risk caused by heavy metals in kiln dust from coal-fired clay brick factories in Türkiye. *Expodure and Health*. https://doi.org/10.1007/s12403-024-00662-4

Turhan, Ş, Çeter, T., Altuner, E. M., Karabıcak, S., Çeter, S., Bıyıklıoğlu, O., Aktaş, Ş, & Kurnaz, A. (2024). Determination of potentially toxic metals and natural radionuclides in airborne pollens produced different urban environments in Turkey and health risk assessment. *International Journal of Environmental Health Research*. https://doi.org/10.1080/09603123.2024.2391460

Turhan, Ş, Köse, A., Varinlioğlu, A., Şahin, N. K., Arıkan, İ, Oğuz, F., Yücel, B., & Özdemir, T. (2012). Distribution of terrestrial and anthropogenic radionuclides in Turkish surface soil samples. *Geoderma, 187–188*, 117–124.

Turhan, Ş, Parmaksız, A., Köse, A., Yüksel, A., Arıkan, İH., & Yücel, B. (2010). Radiological characteristics of pulverized fly ashes produced in Turkish coal-burning thermal power plants. *Fuel, 89*(12), 3892–3900.

UNSCEAR (United Nations Scientific Committee on the Effects of Atomic Radiation). (2000). *Sources and effects of ionizing radiation* (p. 2000). United Nations Publication.

UNSCEAR (United Nations Scientific Committee on the Effects of Atomic Radiation). (2008). *Sources and effects of ionizing radiation* (p. 2010). United Nations Publication.

USEPA (United States Environmental Protection Agency) (2011) Exposure Factors Handbook (Final Report). Chapter 5: Soil and Dust Ingestion. U.S. Environmental Protection Agency, Washington, DC.

Wong, Y. K., Chan, W. W., Gu, D., Wong, T. W., Chan, K. J. D., Yu, J. Z., & Lau, A. K. H. (2023). Characterization of toxic air pollutants in Hong Kong, China: Two-decadal trends and health risk assessments. *Atmospheric Environment, 314*, 1–11.

Yesilkanat, C. M., & Kobya, Y. (2021). Spatial characteristics of ecological and health risks of toxic heavy metal pollution from road dust in the Black Sea coast of Turkey. *Geoderma Regional, 25*, 1–16.

Zakaly, H. M. H., Abbasi, A., Almousa, N., & Savaşan, A. (2024). Naturally occurring radioactive materials (NORM) concentration and health risk assessment of aerosols dust in Nicosia, North Cyprus. *Journal of Radioanalytical and Nuclear Chemistry, 333*, 1073–1082.

Zivuku, M., Kgabi, N. A., & Tshivhase, V. M. (2023). Assessment of radioactivity in particulate matter and soil from selected mining towns of Erongo region, Namibia. *Scientific African, 20*, 1–10.